Ann. Geophysicae 15, 1422–1428 (1997) © EGS – Springer-Verlag 1997

Annales Geophysicae

The effect of vibrationally excited nitrogen on the low-latitude ionosphere

B. Jenkins, G. J. Bailey, A. E. Ennis, R. J. Moffett

Upper Atmosphere Modelling Group, School of Mathematics and Statistics, University of Sheffield, Sheffield S3 7RH, UK

Received: 18 December 1996 / Revised: 14 April 1997 / Accepted: 6 June 1997

Abstract. The first five vibrationally excited states of molecular nitrogen have been included in the Sheffield University plasmasphere ionosphere model. Vibrationally excited molecular nitrogen reacts much more strongly with atomic oxygen ions than ground-state nitrogen; this means that more O^+ ions are converted to NO^+ ions, which in turn combine with the electrons to give reduced electron densities. Model calculations have been carried out to investigate the effect of including vibrationally excited molecular nitrogen on the low-latitude ionosphere. In contrast to mid-latitudes, a reduction in electron density is seen in all seasons during solar maximum, the greatest effect being at the location of the equatorial trough.

1 Introduction

Vibrational excitation of molecular nitrogen molecules is an important factor in the O^+ chemistry of the ionosphere, especially at solar maximum. Vibrationally excited nitrogen affects the electron density through the reaction of atomic oxygen ions with neutral molecular nitrogen. Nitrogen molecules in a vibrationally excited state react much more strongly with O^+ ions than with the ground-state nitrogen molecules, converting the O^+ ions to NO^+ ions. As the NO^+ ions recombine with electrons more readily than the O^+ ions, there is a reduction in the electron density. The production of vibrationally excited molecular nitrogen is strongly dependent upon the electron temperature and density. The Sheffield University Plasmasphere-Ionosphere Model, SUPIM (Bailey *et al.*, 1993; Bailey and Balan, 1996a) has been enhanced to include vibrational excitation of molecular nitrogen. Previous studies of the effects of vibrationally excited molecular nitrogen have concentrated on the mid-latitude ionosphere (Richards and Torr, 1986; Ennis *et al.*, 1995). In the present paper, the low-latitude ionosphere is considered.

At the geomagnetic equator the geomagnetic field $\boldsymbol{B}$, is horizontal, and the plasma undergoes $\boldsymbol{E} \times \boldsymbol{B}$ drift. During the day the plasma drifts upwards. This plasma subsequently diffuses downwards along the field lines under gravity to higher latitudes and causes the crests of the equatorial anomaly to develop. For reviews of experimental and modelling work on the equatorial anomaly see Rajaram (1977), Moffett (1979), Walker (1981), Stening (1992) and Bailey *et al.* (1996). Recent modelling work by Balan and Bailey (1995) and Bailey and Balan (1996b) studied the plasma fountain and the equatorial anomaly in the ionosphere over Jicamarca under equinoctial conditions for moderate solar activity. The effect of the neutral wind and the $\boldsymbol{E} \times \boldsymbol{B}$ drift was investigated. In this paper the ionosphere over Jicamarca is studied under moderate and high solar activity at the vernal equinox and the June and December solstices to investigate the effect that vibrationally excited nitrogen has on the low-latitude ionosphere.

2 Model description

In SUPIM, coupled time-dependent equations of continuity, momentum and energy balance are solved along closed magnetic field lines between base altitudes of about 130 km in conjugate hemispheres. The outputs are the densities, plasma fluxes and temperatures of the electrons and of the O^+, H^+, He^+, N_2^+, O_2^+ and NO^+ ions. The geomagnetic field is represented by an eccentric dipole, which is defined mathematically by the first eight non-zero terms of the spherical harmonic expansion of the geomagnetic scalar potential with coefficients taken from IGRF95. The plasma is transported along geomagnetic field lines by diffusion and neutral winds and in addition is moved perpendicular to the field lines by $\boldsymbol{E} \times \boldsymbol{B}$ drift (Kendall and Pickering,

Correspondence to: B. Jenkins now at British Antarctic Survey, NERC, Madingley Road, Cambridge, CB3 0ET, UK

1967). The $\boldsymbol{E} \times \boldsymbol{B}$ drift acts in such a way that all the charged particles associated with a particular magnetic flux tube are moved into a new magnetic flux tube. The tube of plasma undergoes an expansion or a compression as its apex altitude is increased or decreased. The calculations are solved in a coordinate frame moving with the $\boldsymbol{E} \times \boldsymbol{B}$ drift velocity, so many tubes of plasma are considered. In the present study the model equations are solved along 91 magnetic field lines to give reasonable data coverage over 24 h within the region $\pm 30^\circ$ latitude and 200–2000-km altitude. The neutral atmosphere temperatures and densities are determined from MSIS-86 (Hedin, 1987); however, NO is not included in this empirical model and so its density, $N(\mathrm{NO})$, is calculated from the empirical relationship between the densities of O, O_2 and the neutral temperature, T_n, (Mitra, 1968):

$$N(\mathrm{NO}) = 0.4 \exp(-3700/T_n) N(\mathrm{O})_2 + 5.0 \times 10^{-7} N(\mathrm{O})$$

The neutral wind velocity is determined from HWM90 (Hedin *et al.*, 1991), and the solar EUV fluxes from EUV94, a revised version of EUV91 (Tobiska, 1991). Recently SUPIM has also been enhanced to include a more rigorous calculation of the photoelectron heating adapted from the method of Torr *et al.* (1990). In the model, ionisation is produced by photoionisation of the neutral gases; it is also produced and lost in chemical reactions between ions and neutrals. Diffusion and neutral winds transport the plasma into different regions. The diffusion and reaction-rate coefficients, collision frequencies, cross-sections, heating and cooling rates together with a detailed description of the method of solution have been described elsewhere (Bailey and Balan, 1996a).

The vertical $\boldsymbol{E} \times \boldsymbol{B}$ drift velocity model used in the present study is constructed from measurements made at Jicamarca and from results of previous studies. In the model, the vertical velocity at the magnetic equator is taken from an average drift pattern constructed by Fejer *et al.* (1991) from measurements made at Jicamarca, with an altitude dependence based on the observations of Pingree and Fejer (1987), the theoretical work of Murphy and Heelis (1986) and the modelling study of Su *et al.* (1995). The Jicamarca drift pattern is used for field lines with apex altitude less than 450 km; the drift velocity is assumed to be zero for field lines with apex altitude greater than 3000 km and a linear interpolation is used for intermediate field lines. The zonal component of the $\boldsymbol{E} \times \boldsymbol{B}$ drift velocity is not included in the model calculations as this is thought to have only a negligible effect on the plasma densities (Anderson, 1981). In any event, inclusion is not expected to affect the conclusions of the present study. Temporal plots of the vertical $\boldsymbol{E} \times \boldsymbol{B}$ drift used in the model calculations are shown in Fig. 1; the drifts shown are for summer, winter and equinox (southern hemisphere) for high solar activity. It can be seen that the drift is upward during the day and downward at night. After sunrise, the drift increases steadily upward during the morning, reaching a peak before noon. At this time, the largest drifts are seen at equinox and the smallest in December. The drift then decreases, but before becoming downward at around sunset there is a sudden and sharp increase (the prereversal enhancement). This feature is observed mainly in December and equinox. The drift then remains downward for the rest of the night.

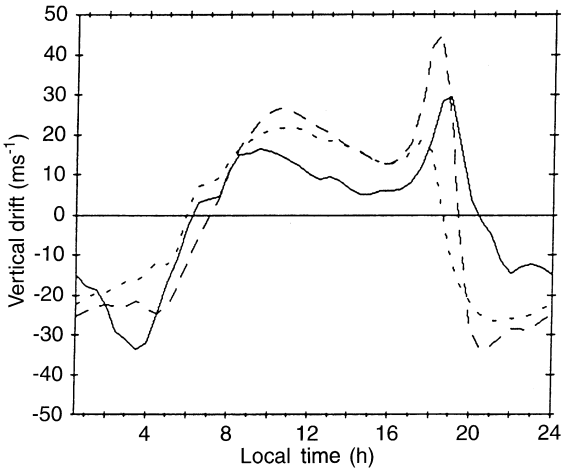

Fig. 1. F-region vertical $\boldsymbol{E} \times \boldsymbol{B}$ drift velocity patterns used in the model at the magnetic equator during solar maximum: *solid lines*: December; *dotted lines*: June, and *dashed lines*: equinox

2.1 The inclusion of vibrationally excited nitrogen

Vibrationally excited nitrogen affects the electron density through the reaction of nitrogen molecules with oxygen ions:

$$\mathrm{O}^+ + \mathrm{N}_2(v) \rightarrow \mathrm{NO}^+ + \mathrm{N}. \quad (1)$$

The rate of this reaction is strongly dependent on the vibrational state, v, the higher the vibrational state the greater being the rate (Schmeltekopf *et al.*, 1967). Thus, more O^+ is converted to NO^+ and the electron density decreases in the presence of vibrationally excited nitrogen, as NO^+ combines with electrons more readily than does O^+ through the reaction

$$\mathrm{NO}^+ + \mathrm{e} \rightarrow \mathrm{N} + \mathrm{O}. \quad (2)$$

SUPIM has been enhanced to include the first five vibrational states of molecular nitrogen. At mid-latitudes the continuity and diffusion equations for the first five vibrationally excited states of molecular nitrogen could be solved along a magnetic field line because at mid-latitudes the F region can be considered to be horizontally stratified (Ennis *et al.*, 1995). However, at low latitudes the equations describing molecular nitrogen have to be solved on a vertical grid. In practice this means that for each time-step of the calculation the ion and electron densities, fluxes and temperatures are solved as before along the magnetic field lines, these values are then interpolated onto the vertical grid on which the densities of the first five vibrationally excited states of molecular nitrogen are solved. These densities are then interpolated back onto the geomagnetic field lines to calculate the ion and electron values at the next time-step. If $N(v)$ is the density of N_2 molecules in

vibrational state v, then the continuity equation for $N(v)$ is

$$\frac{\partial N(v)}{\partial t} + \nabla \cdot \phi(v) = P_v - L_v \tag{3}$$

where $\phi(v)$, P_v and L_v are, respectively, the flux of molecules, the production and loss rates, of $N(v)$. Assuming that transport or diffusion occurs only in the vertical direction (z) then

$$\phi(v) = -D(v)\left(\frac{\partial N(v)}{\partial z} + \frac{N(v)}{T_n}\frac{\partial T_n}{\partial z} + \frac{N(v)}{H}\right), \tag{4}$$

where T_n is the neutral temperature, H is the scale height of N_2 and D is the average molecular diffusion coefficient assumed to be independent of the vibrational state. It is given by Pavlov (1988) as:

$$D = \left(\sum_{\mathrm{X}} \frac{N(X)D_{N_2-X}^{-1}}{N(\mathrm{O}) + N(\mathrm{O_2}) + N(\mathrm{N_2})}\right)^{-1} \tag{5}$$

where $N(X)$ is the density of the Xth constituent ($\mathrm{O}, \mathrm{O_2}$ or $\mathrm{N_2}$) and $D_{N_2-\mathrm{X}}$ is the mutual diffusion coefficient between N_2 and X. The mutual diffusion coefficients for D_{N_2-O} and $D_{N_2-O_2}$ are given by Colegrove *et al.* (1966) and $D_{N_2-N_2}$ by Pavlov (private communication). Equations (3) and (4) are then solved using an implicit finite difference scheme for the first five vibrationally excited states of molecular nitrogen. Chemical equilibrium is assumed at the base altitude of 110 km and diffusive equilibrium is assumed above an altitude of 1000 km. Diffusion is the dominant loss process above 400 km; it acts to transport the vibrationally excited molecules to lower altitudes where the chemical loss rate is greater. This is also the case at mid-latitudes (Richards *et al.*, 1986; Pavlov, 1993).

The reactions involving vibrationally excited nitrogen that are included in the model are:

$$\mathrm{e(therm)} + \mathrm{N_2}(v = j) \rightarrow \mathrm{N_2}(v = i) + \mathrm{e}, \tag{6}$$

$$0 \leq i, j \leq 5,$$

$$\mathrm{O} + \mathrm{N_2}(v) \rightarrow \mathrm{N_2}(v - 1) + \mathrm{O}, \tag{7}$$

$$\mathrm{N} + \mathrm{NO} \rightarrow \mathrm{N_2}(v = 4) + \mathrm{O}. \tag{8}$$

$\mathrm{N_2}(v = 0)$ is the ground state.

The main source of vibrationally excited nitrogen is through the reaction of molecular nitrogen with thermal electrons as shown in reaction (6). Transitions between any of the states can occur. For excitations from the ground state, the cross-sections of Schulz (1964) multiplied by a normalisation factor (Haddad, 1984) have been used. For transitions between states the cross-sections of Chen (1964) have been used where available, otherwise the formula given by Newton *et al.* (1974) has been used. Production of vibrationally excited nitrogen by photoelectrons is not included as this occurs at a much lower rate (Richards *et al.*, 1986). The rate coefficient of the vibrational-translational energy exchange $\mathrm{N_2}(v = 1) - \mathrm{O}$ was measured by McNeal *et al.* (1974) and can be approximated by the use of the theory of this energy exchange as (Pavlov and Buonsanto, 1996):

$$k_7 = 1.07 \times 10^{-16} \exp(-69.9/T_n^{1/3})\ \mathrm{m^3 s^{-1}} \tag{9}$$

The rate used for reaction (8) is $4.0 \times 10^{-17} m^3 s^{-1}$ (Lee *et al.*, 1978). The probability distribution of $\mathrm{N_2}(v)$ in (8) is given by Phillips and Schiff (1962).

The main loss process of vibrationally excited nitrogen at the altitudes of interest is through collisions with atomic oxygen, as described by reaction (7). This reaction has a cascade effect which redistributes the vibrationally excited nitrogen into its lower vibrational states and hence the reaction is both a source and a sink of vibrationally excited nitrogen. The reaction of vibrationally excited nitrogen with thermal electrons (6) also acts as both a source and a sink: the reaction redistributes the nitrogen into the different vibrational states.

Vibrationally excited nitrogen reacts with the atomic oxygen ions as shown by reaction (1). Loss rates for each vibrational state with $\mathrm{O^+}$ are calculated by multiplying the ground-state rate (St-Maurice and Torr, 1978) by the ratios calculated by Schmeltekopf *et al.* (1968). An enhancement factor for the reaction rate of $\mathrm{O^+}$ ions with $\mathrm{N_2}$ is then calculated (Richards and Torr, 1986):

$$f = \sum_{j=0}^{5} k_j N(v_j)/k_0 N(0) \tag{10}$$

The reaction rate is obtained by multiplying the ground-state reaction rate, k_0 by this factor, f. It is this increase in the reaction rate of $\mathrm{O^+}$ with $\mathrm{N_2}$ that reduces the electron density. Since reaction (1) leads to an increase in $\mathrm{NO^+}$ which, in turn, through reaction (2), leads to a decrease in the electron density.

Reaction (6) leads to an energy transfer between the electrons and molecular nitrogen which is included in the electron energy balance equation. The cooling rate is dependent upon the vibrational state of the molecule (Pavlov and Buonsanto, 1996):

$$Q_{en}^{vib} = E_1 N_e \sum_{j=1}^{5} Q_j (N(0) - N(v_j)\exp(jE_1/T_e)) \tag{11}$$

where $\log Q_j = a_j + b_j T_e + c_j T_e^2 - 16$; the constants a_j, b_j and c_j for the vibrational levels $j = 1 - 5$ are given by Pavlov (1988) and E_1 is the energy of the first vibrational level. However, there were no significant differences between results calculated using this rate and results calculated using the usual expression derived by Stubbe and Varnum (1972). This is due to the fact that most of the molecular nitrogen resides in the ground state. At mid-latitudes electron-ion cooling is the dominant cooling channel above 200 km at solar maximum (Richards *et al.*, 1986) and the O fine structure cooling rate is greater than the vibrational nitrogen cooling rate. This is found to be true at low latitudes except for within $\pm 5^\circ$ of the magnetic equator. In the equatorial trough the ionisation decreases and the electron-ion cooling rate is now only dominant above 300-km altitude. Below this altitude cooling to vibrational nitrogen is dominant.

3 Model results and discussion

Sets of calculations, which include and exclude vibrationally excited nitrogen, N_2^*, have been carried out. For each set the same model input parameters were used. The effects of N_2^* are determined by comparing the results of each set. To investigate the seasonal dependence, model calculations have been performed at solar maximum ($F10.7 = 200$), at the vernal equinox and at the December and June solstices. For each calculation the appropriate $\boldsymbol{E} \times \boldsymbol{B}$ drift was used (see Fig. 1).

An example of the altitude profiles of the calculated density of vibrationally excited nitrogen for each of the five states at 1200 LT at the magnetic equator is shown in Fig. 2. These profiles are for December solstice with $F10.7 = 200$. Also shown for comparison is the density of molecular nitrogen given by the MSIS-86 empirical model. This figure shows that the densities decrease rapidly with altitude and that the majority of the excited molecules reside in the first vibrational state at all altitudes. At an altitude of 300 km, less than 10% of the molecules are in the excited state. The presence of vibrational nitrogen reduces the electron density and increases the electron temperature, which in turn causes more vibrationally excited nitrogen to be produced. This positive feedback effect further reduces the electron density and increases the electron temperature (Richards and Torr, 1986). There is a slight maximum in the density of vibrationally excited nitrogen at the magnetic equator; this is due to the reduction in electron density in the equatorial trough and the subsequent increase in electron temperature.

Altitude profiles of the electron density at 1200 LT at the magnetic equator are shown in Fig. 3a. This figure shows that vibrationally excited nitrogen reduces the electron density at both solstices at equatorial latitudes; the decrease is primarily below and at the level of the F2 peak, causing hmF2 to rise. For each season the electron density is reduced by a third at an altitude of 350 km. Figure 3b shows altitude profiles of electron density at $+15°$ magnetic latitude at the vernal equinox and at the December and June solstices. Again there are reductions in electron density mainly at or below the F2 peak; the electron density at 300-km altitude is reduced by about a fifth in each season. This is in contrast to mid-latitudes where the reduction in winter is negligible (Ennis *et al.*, 1995).

The corresponding electron temperature profiles are shown in Fig. 4. At the magnetic equator, the electron density is greater in December than in June, but the electron temperature is higher in June than in December. So, because the production of vibrationally excited nitrogen is dependent upon both electron density and temperature, the effect of vibrationally excited nitrogen is seen during all seasons. At $+15°$ magnetic latitude the magnitude of the peak in electron density varies little with season, but the altitude of the peak is greater at the June solstice. This means that below an altitude of 400 km the greatest electron densities are found in the winter hemisphere, but the highest electron temperatures are found in the summer hemisphere. This is in agreement with the behaviour at mid-latitudes. How-

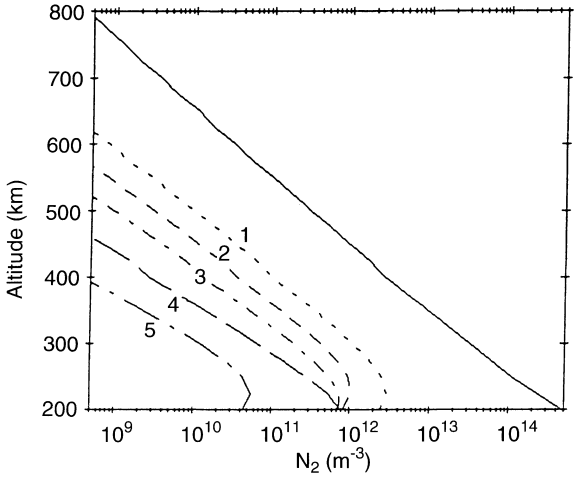

Fig. 2 Modelled altitude profiles at the magnetic equator at noon of the densities of the first five vibrationally excited states of nitrogen; together with the density of molecular nitrogen from MSIS-86 shown by the *solid line*. Results are for the December solstice, F10.7 = 200

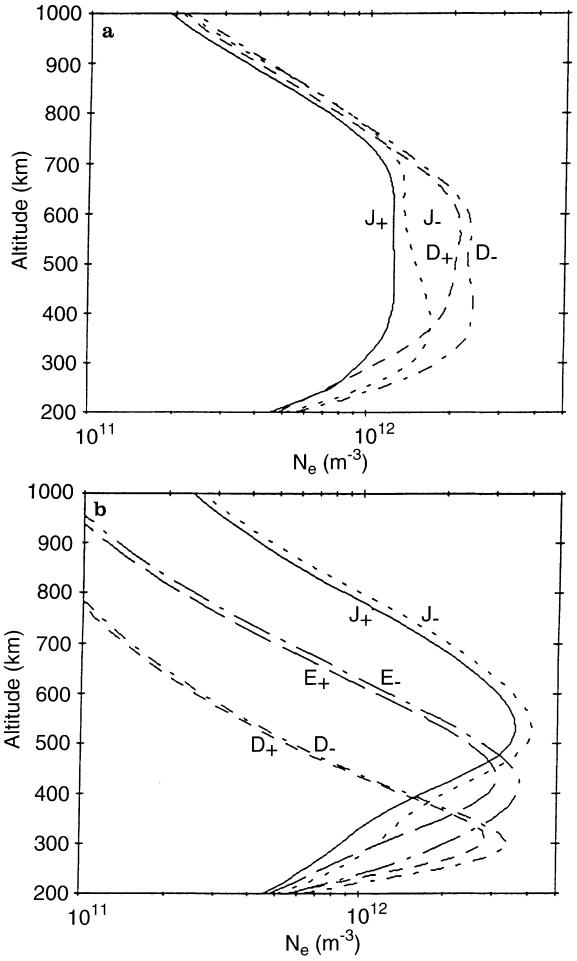

Fig. 3. a, b. Modelled electron density profiles at noon with (+), and without (-) N_2^* for the December (D) and June (J) solstices; **a** at the magnetic equator; **b** at $+15°$ magnetic latitude; this figure also shows the profiles modelled for equinox (E)

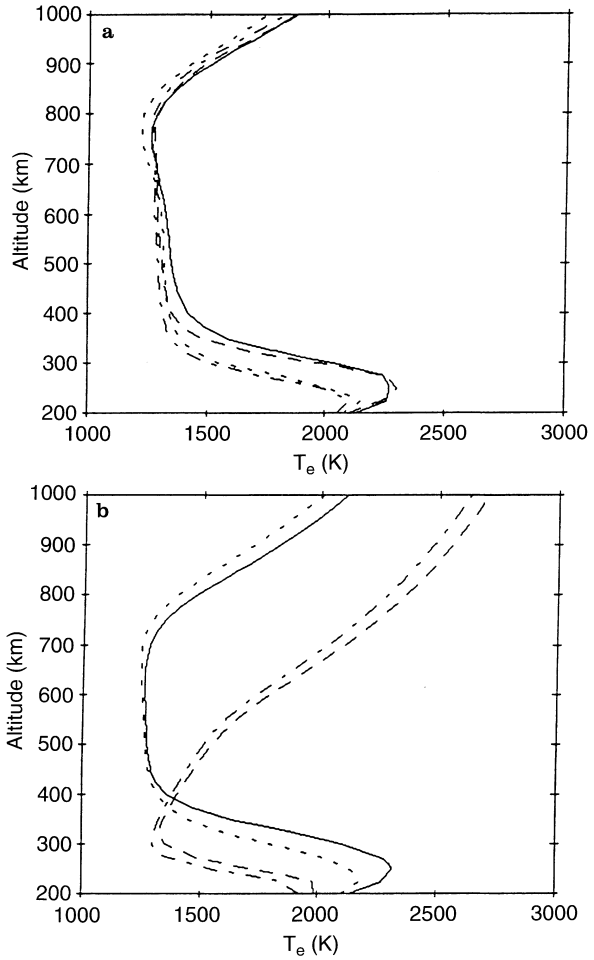

Fig. 4.a, b Modelled electron temperature profiles at noon with and without N_2^* for the December and June solstices; **a** at the magnetic equator; **b** at $+15°$ magnetic latitude; curves are as in Fig. 5

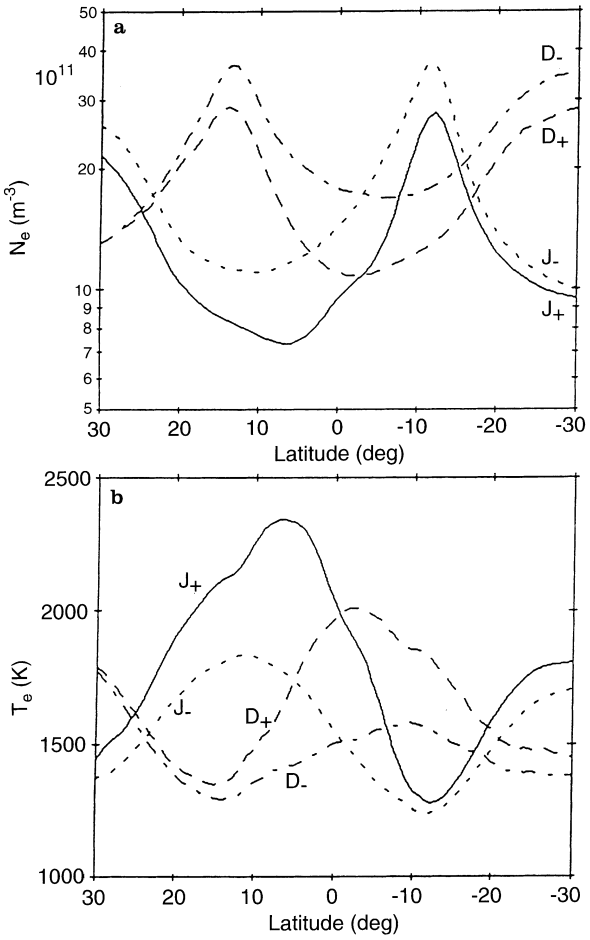

Fig. 5.a Modelled electron density and **b** modelled electron temperature as a function of latitude at noon at 300 km with (+) and without (–) N_2^* for the December (D) and June (J) solstices

ever, above 400-km altitude the situation is reversed, with the highest electron temperatures in the winter hemisphere and the greatest electron densities in the summer hemisphere; this agrees with the Hinotori satellite measurements presented by Su *et al.* (1995). This means that vibrationally excited nitrogen is produced during all seasons at low latitudes, causing a reduction in electron density all year round.

Figure 5 displays the electron density and temperature at 300-km altitude as a function of latitude at 1200 LT at the December and June solstices. At each solstice, the densities at $\pm 30°$ are greatest in the summer hemisphere and lowest in the winter, but equatorwards of this latitude the reverse is true, with the greatest electron densities at 300-km altitude in the winter hemisphere. The equatorial trough and anomaly crests in electron density are clearly seen. There is a reduction in electron density due to the inclusion of vibrational nitrogen at all latitudes. The largest reduction is at the latitudes of the equatorial trough, since the reduction in electron density produces an increase in electron temperature which, in turn, causes more vibrationally excited nitrogen to be produced. The magnitude of the reduction decreases polewards of the trough and is very small in the winter hemisphere, in agreement with results from mid-latitudes (Richards *et al.*, 1986; Ennis *et al.*, 1995). At equinox the magnitude of the electron density is intermediate to the summer and winter values in each hemisphere, and the reduction due to the presence of vibrational nitrogen is again greatest in the equatorial trough. The highest electron temperatures at 300-km are predicted to be in the summer hemisphere, the presence of vibrationally excited nitrogen increases the temperature by about 500 K at the latitude of the equatorial trough. This is due to the low electron density of the June hemisphere at this altitude.

Model results have confirmed the fact that the effect of vibrationally excited nitrogen does increase with solar activity. This can be seen in Fig. 6, which shows electron density profiles modelled for the December solstice under moderate solar activity conditions ($F10.7 = 120$). In this case the inclusion of vibrationally excited nitrogen reduces the electron density only by a tenth. This is in agreement with results at mid-latitudes (Richards and Torr, 1986).

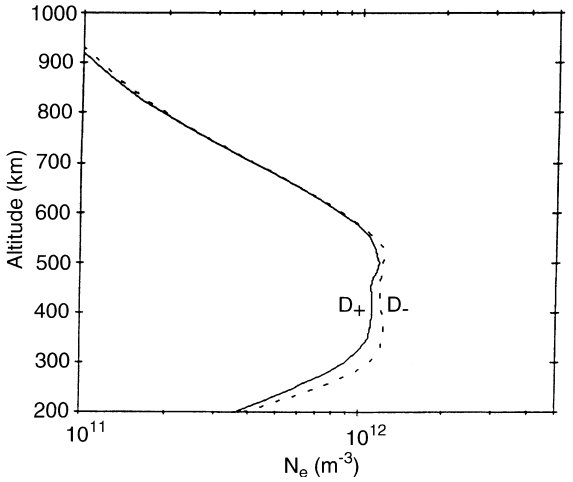

Fig. 6. Modelled electron density profiles at the magnetic equator at noon with (+), and without (–) N_2^* for the December solstice; $F10.7 = 120$

4 A comparison with experimental data

Exact simulations of observations are not attempted. The values of the drifts and winds used in the model computations are averages for the chosen seasons and the day-to-day variability of the $\boldsymbol{E} \times \boldsymbol{B}$ drifts and the neutral winds will affect the measurements. To show possible trends, an example of Jicamarca data from the CEDAR database is presented in Fig. 7. This compares model and incoherent-scatter electron densities for noon local time in December for solar maximum conditions. Vibrationally excited nitrogen affects the electron density mainly below 400-km altitude; a comparison of the modelled and measured values in this region does indicate that vibrationally excited nitrogen might be important.

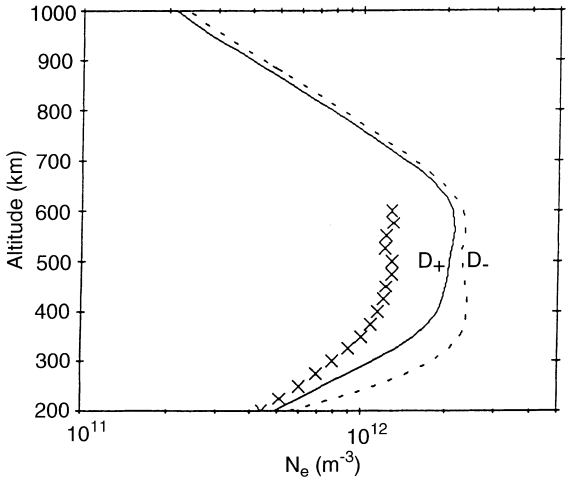

Fig. 7. Modelled electron density profiles at the magnetic equator at noon with (+) and without (–) N_2^* for the December solstice; also shown are measurements from Jicamarca (×) for noon on 21 December 1967; $F10.7 = 200$

5 Summary

SUPIM, the Sheffield University Plasmasphere Ionosphere Model, has been enhanced to include the first five vibrational states of molecular nitrogen. The enhanced model has been used to investigate the effect of vibrationally excited molecular nitrogen, N_2^*, on the low-latitude ionosphere. Model calculations show that N_2^* affects the electron density through reactions (1) and (2); reaction (1) is strongly dependent on the vibrational state of the nitrogen molecule, the higher the state the greater the reaction rate. The model calculations predict that the majority of the excited molecules reside in the first vibrational level, but sufficient numbers reside in the upper levels to enhance the reaction rate. This means that more NO^+ ions are produced when vibrationally excited nitrogen is present, and these, in turn, combine with the electrons to reduce the electron density. The production of vibrationally excited nitrogen is dependent on the electron density and temperature. Generally, the higher the electron temperature the more vibrational nitrogen is produced. Thus, the density is greater at solar maximum. More N_2^* is produced in the daytime than at night, and more at latitudes close to the equator than further away.

The effect of vibrational nitrogen is to reduce the electron density. The reduction increases with solar activity and is most marked at the latitude of the equatorial trough, though there is a significant reduction at the crests of the equatorial anomaly. The reduction is greatest below and at the altitude of the F-region peak causing hmF2 to rise. In contrast to mid-latitudes, there is a significant reduction in electron density in all seasons. The reduction in electron density causes the electron temperature to rise, thus causing more vibrationally excited nitrogen to be produced and a lowering of the electron density. At low latitudes the highest electron temperatures occur in the hemisphere opposite to the highest electron densities. Thus, although the electron densities are low, the electron temperatures are high, which means that significant quantities of vibrationally excited nitrogen are produced and the electron density is reduced. In the opposite hemisphere the electron temperature is low but the electron density is higher and so vibrational nitrogen is again produced and the electron density is reduced by about the same amount.

Comparisons with electron density and temperature incoherent-scatter measurements at Jicamarca do, perhaps, show that the data agree better with the model results which include vibrationally excited nitrogen. An exact simulation of the data was not attempted, as other factors such as the variability of the $\boldsymbol{E} \times \boldsymbol{B}$ drift will also affect the results.

Vibrationally excited nitrogen can have significant effects on the low-latitude ionosphere, particularly at solar maximum. In the equatorial trough the presence of vibrational nitrogen can cause the electron density to be reduced to two-thirds of its value when vibrational nitrogen is absent.

Acknowledgements. This work was supported by PPARC, UK under grants: GR/K06112 and GR/L20238. One of us (AEE) was supported by a PPARC studentship. The incoherent-scatter data from Jicamarca were obtained through the CEDAR database supported by NSF, USA.

Topical Editor D. Alcaydé thanks A. V. Pavlov and P. -L. Blelly for their help in evaluating this paper.

References

Anderson, D. N., Modelling the ambient, low-latitude F-region ionosphere - a review, *J. Atmos. Terr. Phys*., **43,** 753, 1981.

Bailey, G. J., and N. Balan, A low-latitude ionosphere-plasmasphere model, in *STEP Handbook on Ionospheric Models*, *Ed. R. W. Schunk, Utah State University*, **173,** 1996a.

Bailey, G. J., and N. Balan, Some modelling studies of the equatorial ionosphere using the Sheffield University Plasmasphere ionosphere model, *Adv. Spac Res*., **18(6),** 59, 1996b.

Bailey, G. J., R. Sellek, and Y. Rippeth, A modelling study of the equatorial topside ionosphere, *Ann. Geophys*, **11,** 263, 1993.

Bailey, G. J., N. Balan, and Y. Z. Su, The Sheffield University ionosphere plasmasphere model – a review, *J. Atmos. Terr. Phys*., 1996.

Balan, N, and G. J. Bailey, Equatorial plasma fountain and its effects: possibility of an additional layer, *J. Geophys. Res*., **100,** 21421, 1995.

Chen, J. C. Y., Theory of subexcitation electron scattering by molecules. 2. Excitation and de-excitation of molecular vibration, *J. Chem. Phys*., **40,** 3513, 1964

Colegrove, F. D., F. S. Johnson, and W. B. Hanson, Atmospheric composition in the lower thermosphere, *J. Geophys. Res*., **71,** 2227, 1966.

Ennis, A. E., G. J. Bailey, and R. J. Moffett, Vibrational nitrogen density in the ionosphere and its dependence on season and solar cycle, *Ann. Geophys*, **13,** 1164, 1995.

Fejer, B. G., E. R. de Paula, S. A. Gonzales, and R. F. Woodman, Average vertical and zonal F-region plasma drifts over Jicamarca, *J. Geophys. Res*., **96,** 13901, 1991.

Haddad, G. N., Cross-section for electron scattering in nitrogen, *Aust. J. Phys*., **37,** 487, 1984.

Hedin, A. E., MSIS-86 thermospheric model, *J. Geophys. Res*., **92,** 4649, 1987.

Hedin, A. E., M. A. Biondi, R. G. Burnside, G. Hernandez, R. M. Johnson, T. L. Killeen, C. Mazaudier, J. W. Meriwether, J. E. Salah, R. J. Sica, R. W. Smith, N. W. Spencer, V. B. Wickwar, and T. S. Virdi, Revised global model of thermosphere winds using satellite and ground-based observations, *J. Geophys. Res*., **96,** 7657, 1991.

Kendall, P. C., and W. M. Pickering, Magnetoplasma diffusion at F2-region altitudes, *J. Atmos. Terr. Phys*., **15,** 825, 1967.

Lee, J. H., J. V. Michael, W. A. Payne, and L. J. Stief, Absolute rate of the reaction of N(4S) with NO from 196–400 K with DF-RF and FP-RF techniques, *J. Chem. Phys*., **69,** 3069, 1978.

McNeal, R. G., M. E. Whitson, and G. R. Cook, Temperature dependence of the quenching of vibrationally excited nitrogen by atomic oxygen, *J. Geophys. Res*., **79,** 1527, 1974.

Mitra, A. P., A review of D-region processes in non-polar latitudes, *J. Atmos. Terr. Phys*., **30,** 1065, 1968.

Moffett, R. J., The equatorial anomaly in the electron distribution of the terrestrial F region, *Fundam. Cosmic Phys*., **4,** 313, 1979.

Murphy, J. A., and R. A. Heelis, Implications of the relationship between the electromagnetic drift components at mid-and low-latitudes, *Planet. Space Sci*., **34,** 645, 1986.

Newton, G. P., J. C. G. Walker, and P. H. E. Meijer, Vibrationally excited nitrogen in stable auroral red arcs and its effect on ionospheric recombination. *J. Geophys. Res*., **79,** 3807, 1974.

Pavlov, A. V., The role of vibrationally excited nitrogen in the ionosphere, *Pure Appl. Geophys*., **127,** 529, 1988.

Pavlov, A. V., The role of vibrationally excited nitrogen in the formation of the mid-latitude ionisation trough, *Ann. Geophysicae*., **11,** 479, 1993.

Pavlov, A. V., and M. J. Buonsanto, Using steady-state vibrational temperatures to model effects of N2* on calculations of electron densities, *J. Geophys. Res*., **101**, 26941, 1996.

Phillips, L. F., and H. I. Schiff, Mass spectrometric studies of atom reactions II. Vibrationally excited N2 formed by the reaction of N atoms with NO, *J. Chem. Phys*., **36,** 3283, 1962.

Pingree, J. E., and B. G. Fejer, On the height variation of the equatorial F-region vertical plasma drifts, *J. Geophys. Res*., **92,** 4763, 1987.

Rajaram, G., Structure of the equatorial F region, topside and bottomside—a review, *J. Atmos. Terr. Phys*., **39,** 1125, 1977.

Richards, P. G., and D. G. Torr, A factor of 2 reduction in theoretical F2 peak electron density due to enhanced vibrational excitation of N_2 in December at solar maximum, *J. Geophys. Res*., **91,** 11331, 1986.

Richards, P. G., D. G. Torr, and W. A. Abdou, Effects of vibrational enhancement of N_2 on the cooling rate of ionospheric thermal electrons. *J. Geophys. Res*., **91,** 304, 1986.

Schmeltekopf, A. L., F. C. Fehsenfeld, G. I. Gilman, and E. E. Ferguson, Reaction of atomic oxygen ions with vibrationally excited nitrogen molecules, *Planet. Space Sci*., **15,** 401, 1967.

Schmeltekopf, A. L., E. E. Ferguson, and F. C. Fehsenfeld, Afterglow studies of the reactions of He^+, $He(2^3S)$ and O^+ with vibrationally excited N_2,*J. Chem. Phys*., **48,** 2966, 1968.

Schulz, G. J., Vibrational excitation of N_2, CO, and H_2 by electron impact, *Phys. Rev*., **135,** A988, 1964.

St-Maurice, J. P., and D. G. Torr, Nonthermal rate coefficients in the ionosphere: the reactions of O^+ with N_2, O_2 and NO, *J. Geophys. Res*., **83,** 969, 1978.

Stening, R. J., Modelling the low-latitude F region, *J. Atmos. Terr. Phys*. , **57,** 433, 1992.

Stubbe, P., and W. S. Varnum, Electron energy transfer rates in the ionosphere, *Planet. Space. Sci*., **20,** 1121, 1972.

Su, Y. Z., K. I. Oyama, G. J. Bailey, T. Takahashi, and S. Watanabe, Comparison of satellite electron density and temperature measurements at low latitudes with a plasmasphere-ionosphere model, *J. Geophys. Res*., **100,** 14591, 1995.

Tobiska, W. K., Revised solar extreme ultraviolet flux model, *J. Atmos. Terr. Phys.,* **53**, 1005, 1991.

Torr, M. R., D. G. Torr, P. G. Richards, and S. P. Yung, Mid- and low-latitude model of thermospheric emissions, 1, $O^+(^2P)$ 7320 Å and $N_2(2P)$ 3371 Å, *J. Geophys. Res*., **95,** 21147, 1990.

Walker, G. O., Longitudinal structure of the F-region equatorial anomaly – a review, *J. Atmos. Terr. Phys*., **43,** 763, 1981.